Two-Photon Lasers Based on Intersubband Transitions in Semiconductor Quantum Wells

C. Z. Ning*

Center for Nanotechnology, NASA Ames Research Center, Mail Stop N229-1, Moffett Field, California 94035, USA
(Received 22 April 2004; published 28 October 2004)

We propose to make a two-photon laser based on intersubband (sublevel) transitions in semiconductor nanostructures. The advantages and feasibility of such a two-photon laser are analyzed in detail using the density matrix approach. Both one-photon and two-photon gains in a three subband quantum well structure are studied on the same footing to show how the two-photon gain can be maximized, while the competing one-photon gain is minimized. The results show that a sufficient two-photon gain can be achieved to overcome one-photon competition and the loss of a conventional semiconductor cavity, making intersubband transitions one of the very few feasible approaches to two-photon lasing.

A two-photon laser (TPL) is based on stimulated emission of two photons in conjunction with one electronic transition between two states of the same parity and thus not directly connected by a dipole transition. The realization of such a TPL was a dream of the quantum electronics community since its very conception 40 years ago [1]. There is a great deal of interest in making such a TPL: Conceptually, a TPL is a unique device which operates on high order transitions involving virtual states, and thus having no classical counterpart. From laser physics and quantum optics perspectives, TPLs show many interesting features [2,3] that are distinct from their one-photon counterparts. These features include squeezed state operation [4] instead of coherent state operation for the one-photon laser, even though various aspects of quantum statistics are still in need of systematic understanding [5] (for a most recent extensive review, see [3]). Other distinct features include threshold bistability [2,6–8], nonrelaxation Rabi-oscillation [2,7], and higher order instabilities [2,8]. These unique features of TPLs naturally lead to interesting applications not feasible with the usual lasers. TPLs were originally suggested as a widely tunable coherent source in the nondegenerate mode of operation. Many more interesting applications have been proposed such as high precision measurements, laser gyroscope, quantum communication [9], and most recently, the generation of polarization-entangled twin beams [10] (see Ref. [3] for more references).

Because of inherent difficulties associated with higher order (and weaker) transitions and other competing mechanisms, realization of TPL has been an extremely challenging task. So far only two successful demonstrations of continuous-wave operation of TPL have been reported based on driven two-level atoms [11] and 3-level Rydberg states [12]. Both of these realizations use the maser-type approach, namely, inject the well-prepared atom beams into a cavity. Given the potential applications, especially in optical communication with nonclassical light [9], it would be highly desired to make a TPL based on semiconductors due to obvious advantages such

as efficiency, compactness, and ease of use, among many others, of a semiconductor laser. In addition, as we will discuss in the following, intersubband transitions in a properly designed quantum well structure have all the advantages of the Rydberg atoms that made the first cw TPL possible [12]. Finally, a semiconductor TPL would represent a major milestone in our utilization of nonlinear optical processes in semiconductor nanostructures and may open more interesting applications for TPLs. In fact, two-photon gain in a semiconductor based on *interband* transitions was the topic of a few recent investigations [13,14]. However, we believe that TPLs based on *intersubband* transitions are more likely to succeed. The reasons are as follows: The TPL based on Rydberg states of Rb atoms relies on a fortunate convergence of several advantages [12]: the huge dipole moments between dipole allowed states, the availability of an intermediate state that is sufficiently close to the midway between the two dipole-forbidden states, and the possibility of high Q cavity in the microwave regime. Using intersubband transitions, all these advantageous aspects of the Rydberg states can be realized by virtue of nanostructure engineering. In this Letter, we propose a class of TPLs based on intersubband or intersublevel (in the case of quantum dots) transitions in semiconductor nanostructures. Even though the idea and most of the calculations will apply to quantum wells, wires, and dots, our following treatment refers explicitly to quantum well structure for specificity. Our model is a symmetric, step quantum well structure shown in the inset of Fig. 1. The first advantage of the intersubband transitions is the large dipole moments, as large as 10 times the interband dipole moments. This factor alone would lead to a two-photon gain (TPG) 10 000 times [see Eq. (11) in the following] that of interband. Experimentally it was observed that the two-photon intersubband transitions are at least 2 orders of magnitude stronger than the interband transitions [15]. The second advantage of the particular quantum well structure is the almost continuous "tunability" of the one-photon detuning (distance of the midlevel to the
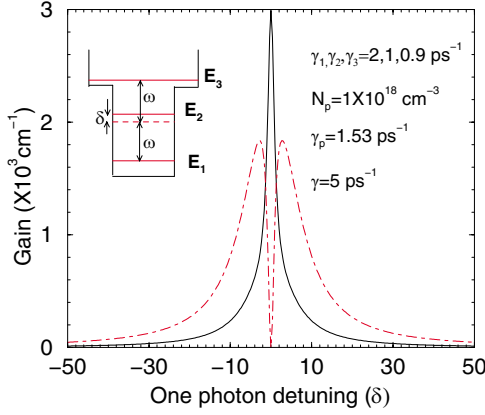
FIG. 1 (color online). G_1 (solid line) and G_2 (dash-dotted line) as a function of the one-photon detuning in a quantum well structure as depicted in the inset. Other parameters are given in the figure $N_p = 2\sum_k f_{pk}/V$.

halfway between the two dipole-forbidden states) by varying the upper state position. This can be achieved through variation of material composition or the width of the layers of the structure. To demonstrate the feasibility of such an intersubband transition based TPL, we will use the density matrix approach, as was done previously for TPLs [2,16]. This approach will allow us to treat the one-photon gain (OPG) and TPG on equal footing for a given model. We will show that the flexibility of the one-photon detuning afforded by our model gives a large TPG than the OPG, thus allowing two-photon lasing for the chosen detuning.

As a model material system, we consider the GaAs/AlGaAs system. The core of the structure consists of three layers: a central layer of GaAs of 14 nm in thickness and two side layers of $Al_{0.1}Ga_{0.9}Al$ of 6 nm each on both sides of the GaAs layer (see the inset of Fig. 1). The band edge separations are: $E_3 - E_2 = 58$ and $E_2 - E_1 = 44$ meV. Although these transition energies are in the far-infrared range, using deeper quantum wells such as InAs/AlGaSb would allow us to scale the photon energy to the midwave infrared range. The dipole matrix elements between states 1 and 2 and between 2 and 3 are almost the same and around 34 eÅ, where e is the charge unit of an electron. As expected, the dipole moment is 0 between 1 and 3, between which two-photon lasing is desired. In the following, we analyze the optical gain using the density matrix equations without the many-body Coulomb interaction. Such Coulomb effects can be included in a straightforward, though a bit complicated, manner along the line of our recent work [17]. Under the rotating wave approximation, the set of equations describing the interaction of a light (probe) field $\mathcal{E} = \mathcal{E}_0 e^{-i\omega t} + \mathcal{E}_0^* e^{i\omega t}$ with an n-type doped quantum well having three subbands is given as follows:

$$\frac{dp_{12k}}{dt} = -\lambda_{12k} p_{12k} - i\Omega_{21}(f_{1k} - f_{2k}) - i\Omega_{32}^* p_{13k}, \quad (1)$$

$$\frac{dp_{23k}}{dt} = -\lambda_{23k} p_{23k} - i\Omega_{32}(f_{2k} - f_{3k}) + i\Omega_{21}^* p_{13k}, \quad (2)$$

$$\frac{dp_{13k}}{dt} = -\lambda_{13k} p_{13k} - i\Omega_{32} p_{12k} + i\Omega_{21} p_{23k}, \quad (3)$$

$$\frac{df_{1k}}{dt} = -\gamma_1 f_{1k} + \gamma_2 f_{2k} - i(\Omega_{12}^* p_{12k} - \text{c.c.}), \quad (4)$$

$$\frac{df_{2k}}{dt} = -\gamma_2 f_{2k} + \gamma_3 f_{3k} + i(\Omega_{12}^* p_{12k} - \text{c.c.})$$
$$- i(\Omega_{23}^* p_{23k} - \text{c.c.}), \quad (5)$$

$$\frac{df_{3k}}{dt} = -\gamma_3 f_{3k} + \gamma_p f_{pk} + i(\Omega_{23}^* p_{23k} - \text{c.c.}), \quad (6)$$

where $\lambda_{lmk} = \gamma_{lm} + i[(E_{mk} - E_{lk})/\hbar - \omega]$ for λ_{12k} and λ_{23k}, while $\lambda_{13k} = \gamma_{13} + i[(E_{3k} - E_{1k})/\hbar - 2\omega]$. $\Omega_{lm} = d_{lm}\mathcal{E}_0/\hbar$ are the Rabi frequencies. d_{lm}'s are the dipole matrix elements. γ_{lm}'s and γ_l's are dephasing rates and population decay rates, respectively. γ_p and f_{pk} are the pump rate and pump Fermi function to state 3. p_{ijk}'s and f_{jk}'s are the intersubband polarization amplitudes and Fermi distributions, respectively. E_{ik} is the energy of subband i defined as $E_{ik} = E_i + \hbar^2 k^2/2m_i$ under the parabolic band approximation and k is the electron wave vector along the unquantized direction.

Since TPG depends on the intensity of the probe field, we will solve the exact steady state solution of Eqs. (1)–(6), without assuming the optical field being weak. The medium (complex) polarization per unit volume (V) is defined as $P = \frac{2}{V}\sum_k[d_{21}p_{12k} + d_{32}p_{23k}]$, which can be further written for steady state as

$$P = -\frac{2i}{V}\sum_k \left[\frac{d_{21}^2(f_{1k} - f_{2k})}{\hbar\lambda_{12k}} + \frac{d_{32}^2(f_{2k} - f_{3k})}{\hbar\lambda_{23k}}\right]\mathcal{E}_0$$
$$- \frac{2i}{V}\sum_k \left[\frac{d_{21}d_{23}}{\hbar\lambda_{12k}} - \frac{d_{12}d_{32}}{\hbar\lambda_{23k}}\right]\mathcal{E}_0 p_{13k}$$
$$\equiv P_1 + P_2, \quad (7)$$

where p_{13k} is given by

$$p_{13k} = \frac{\Omega_{21}\Omega_{32}[\lambda_{12k}(f_{2k} - f_{3k}) - \lambda_{23k}(f_{1k} - f_{2k})]}{\lambda_{12k}\lambda_{23k}\lambda_{13k} + \lambda_{12k}\Omega_{12}^2 + \lambda_{23k}\Omega_{23}^2}. \quad (8)$$

The first term in Eq. (7) is the one-photon polarization due to 1-2 and 2-3 transitions (P_1), while the second term is the two-photon polarization (P_2) between dipole-forbidden states 1 and 3 and is proportional to p_{13k}. Notice that the lowest order of the two-photon polarization is obtained by assuming that the population differences in (8) are constants. From Eq. (8), this leads to $p_{13k} \propto \Omega_{21}\Omega_{32} \propto \mathcal{E}_0^2$, namely, TPG is proportional to the intensity of the probe field at the lowest order of the field. This is in contrast to OPG. To obtain optical polarization or gain, we need to solve population differences in (8)

self-consistently with various off-diagonal components. To obtain some insightful analytical results, we assume that (i) the effective mass differences between the three bands can be ignore: $m_j = m$; (ii) the dipole moments of two transitions are the same: $d_{12} = d_{23} = d$; and (iii) dephasing rates are the same, i.e., $\gamma_{12} = \gamma_{23} = \gamma$. Furthermore, we will only study the case of perfect two-photon tuning, namely, $E_3 - E_1 = 2\hbar\omega$ for simplicity. This leads to a single one-photon detuning parameter defined through $\gamma\delta = (E_{3k} - E_{2k})/\hbar - \omega = \omega - (E_{2k} - E_{1k})/\hbar$. Under these approximations, one-photon and two-photon optical susceptibilities can be written as follows:

$$\chi_1 = \frac{d^2\{\delta[(N_3 - 2N_2 + N_1)] + i[(N_3 - N_1)]\}}{\epsilon_0 n_b^2(1 + \delta^2)(\gamma\hbar)}, \quad (9)$$

$$\chi_2 = \frac{2\mathcal{E}_0^2 d^4 \delta}{\epsilon_0 n_b^2(\gamma\hbar)^3} \frac{2N_2 - N_3 - N_1 + i\delta(N_3 - N_1)}{(1 + \delta^2)[1 + \delta^2 + 2(d\mathcal{E}_0/\gamma\hbar)^2]}, \quad (10)$$

where χ_j's are defined through $P_j = \epsilon_0 n_b^2 \chi_j \mathcal{E}_0$ ($j = 1, 2$). n_b is the refractive index. $N_j = \frac{2}{V}\sum_k f_{jk}$ are the population density of subband j, which have to be solved self-consistently from Eqs. (4)–(6). The optical gain per unit length is defined through $G_j = n_b \frac{\omega}{c} \text{Im}\{\chi_j\}$ ($j = 1, 2$), where Im stands for the imaginary part. It is important to note from (10) that TPG is proportional to the population difference of subbands three and 1. This means that TPG is due to the incoherent population inversion, and not due to any coherent parametric processes. The role of the middle level can be clearly understood from Eq. (10). In the limit of small linewidth broadening and at the lowest order of the probe field, the two-photon gain can be approximated as

$$G_2 = \frac{2d^4\mathcal{E}_0^2\omega}{\epsilon_0 n_b c \gamma^3 \hbar^3} \frac{N_3 - N_1}{\delta^2}. \quad (11)$$

Several important observations can be made: First, TPG is proportional to the quartic of dipole moments. This is why large dipole moments between the middle state and the two dipole-forbidden states are so important. Second, the inverse quadratic dependence on one-photon detuning is the reason why a middle state with a variable detuning δ is important to increase TPG, as originally proposed by Brune et al. [12]. However, it is important to realize that this conclusion is valid only when the linewidth broadening is small, and much smaller than the detuning. In semiconductors, the linewidth can be as large as a few meV. The approximate formula for the TPG is only valid when $\delta \gg 1$, $d\mathcal{E}_0/\gamma\hbar$.

An important relation, the ratio of TPG to OPG, can be obtained from Eqs. (9) and (10)

$$\frac{G_2}{G_1} = 2\left(\frac{d\mathcal{E}_0}{\gamma\hbar}\right)^2 \frac{\delta^2}{1 + \delta^2 + 2(d\mathcal{E}_0/\gamma\hbar)^2}. \quad (12)$$

We see that the gain ratio increase with probe field power

and the one-photon detuning. The TPG approaches zero when either the detuning or the probe power goes to zero. The gain ratio saturates when either of them goes large.

In the following, we present numerical results for more general situations by solving Eqs. (1)–(6). Figure 1 shows the general features of OPG and TPG in a three subband system. As expected, OPG shows the usual Lorentzian behavior peaked at zero detuning. TPG shows a double-peak structure and is at the minimum for zero detuning. To the best of our knowledge, this double-peak feature has not been noticed in all the earlier papers. With the further increase of the one-photon detuning, the TPG reaches maximum and gradually overtakes OPG. At sufficiently large detuning, TPG start to decrease. The enhancement of TPG through the middle level is also obvious. The flexibility with the step quantum well (inset of Fig. 1) in designing such detuning assures that we can always maximize the difference between TPG and OPG.

Figure 2 shows OPG (top), TPG (middle) and the ratio of the two (bottom) as function of the detuning at various levels of the probe field power. OPG decreases monotonously because of the decrease of the population inversion as a result of increased absorption of the probe field. TPG increases initially with the increase of the probe field power, which is accompanied by an increase in the peak detuning. With sufficiently strong probe power, TPG is saturated, and then reduced (compare curve three with four in the middle panel) as can be seen from Eq. (10). [Notice that the populations also changes with probe power in (10)]. Because of the similar reduction of both TPG and OPG with increasing probe power, the ratio of the two approaches a constant value asymptotically, as seen in the bottom panel of Fig. 2. Figure 2 shows that, with a proper choice of the one-photon detuning, we can achieve a desired amount of TPG in excess of OPG depending on the cavity loss.
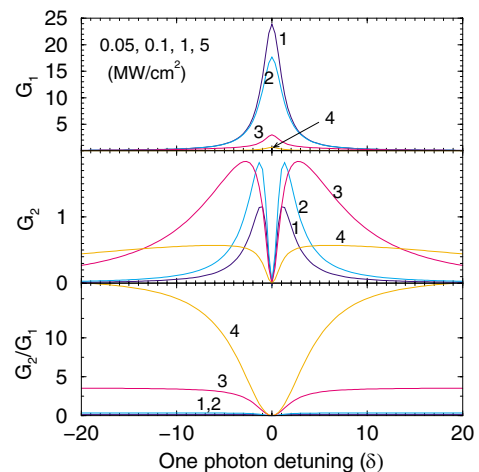
FIG. 2 (color online). Optical gain and gain ratio as a function of the one-photon detuning for various probe power levels as given in the top panel, marked, respectively, by 1 through 4 in the increasing order.
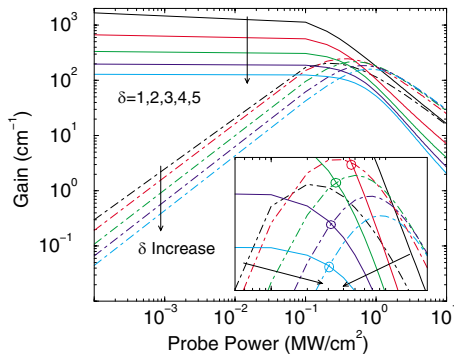
FIG. 3 (color online). G_1 (solid line) and G_2 (dash-dotted line) as functions of the probe field power as δ is increased from one through five in the order indicated by the arrow. The inset shows the enlarged section where G_2 overtakes G_1. The crossing point at each detuning is marked by a circle.

Figure 3 shows TPG and OPG as a function of probe power at several detuning values. As expected, TPG is proportional to the probe power, while OPG is power independent at low power level. Initially OPG is larger. At a sufficiently high probe power (called critical power), TPG start to overtake OPG for a sufficiently large detuning. Thereafter OPG decreases faster than TPG with increasing probe power. Within the range of parameters shown in Fig. 3, we see that the larger the detuning is, the smaller such critical power level is. This leads to a recipe for the two-photon laser design: For a given laser cavity design, we know the threshold TPG. From this gain requirement, we can decide on a detuning parameter, which in turn determines the exact quantum well design. For different quantum well designs (width, depth, etc.) we have tried, the dipole moments can vary between 30 and 40 eÅ. TPG varies in the range of a few hundreds to thousands cm^{-1} in the range of detuning where TPG is larger than OPG. Such a gain magnitude is comparable to the typical OPG in the conventional semiconductor lasers. Therefore, it is clear that our TPL proposal combined with usual diode laser cavity design is a feasible approach. We note that the cavity requirement here is not as stringent as for the Rydberg atoms. We can choose a well-detuned midlevel to minimize the OPG, but still have enough TPG (see Fig. 2). For a detuning of $\delta = 5(>2\text{THz})$, the TPG can be as large as 10 times the OPG. Even the same cavity design (same Q) for one-photon and two-photon transitions are chosen, the system will first lase as a TPL. A highly frequency selective cavity with high Q for two-photon resonance and lower Q for the two one-photon transitions will further greatly benefit the two-photon lasing. This can be done through the use of distributed feedback, or distributed Bragg reflector cavities. Photonic crystals (PCs) are another interesting choice. The TPG medium can be sandwiched between two 2D PC slabs. For ω at the center of the PC band gap, we can design a PC band gap narrow enough so that the two one-photon transitions (which are symmet-

rically above and below the ω for exact two-photon resonance) are outside the band gap. This is possible by varying the PC slab parameters [18]. Such a cavity will provide a high quality cavity for two-photon transition, while a very leaky cavity for the one-photon transitions.

In summary, we have proposed a new class of TPLs based on intersubband transitions in semiconductor nanostructures with three subbands (sublevels). Through a detailed theoretical study, we have compared the one- and two-photon gain systematically as function of detuning and probe power levels. We found that for the conventional cavity design, we can always find a combination of detuning and a probe power level such that a threshold gain can be achieved for two-photon lasing, while the competing one-photon lasing can be kept below threshold. We believe that such a TPL is technologically feasible and it may open new applications of TPLs once semiconductor based devices are available. This will also put our understanding of nonlinear optical properties of semiconductor nanostructures to real test to solve one of the challenging issues of quantum electronics.

*Email address: cning@mail.arc.nasa.gov
Electronic address: http://www.nas.nasa.gov/~cning

[1] P. P. Sorokin and N. Braslau, IBM J. Res. Dev. **8**, 177 (1964); A. M. Prokhorov, Science **149**, 828 (1965).
[2] C. Z. Ning, dissertation, University of Stuttgart, 1991.
[3] D. Gauthier, in *Progress in Optics*, edited by E. Wolf (Elsevier Science B.V., Amsterdam, 2003), Vol. 45.
[4] H. P. Yuen, Phys. Rev. A **13**, 2226 (1976).
[5] L. A. Lugiato and G. Strini, Opt. Commun. **41**, 374 (1982); M. D. Reid and D. F. Walls, Phys. Rev. A **28**, 332 (1983); G. Hu and C. Sha, Phys. Lett. A **159**, 47 (1991).
[6] C. Z. Ning and H. Haken, Z. Phys. B **77**, 157 (1989).
[7] H. Concannon and D. Gauthier, Opt. Lett. **19**, 472 (1994).
[8] C. Z. Ning and H. Haken, Z. Phys. B **77**, 163 (1989); E. Roldan *et al.*, Opt. Commun. **104**, 85 (1993).
[9] H. P. Yuen and J. H. Shapiro, IEEE Trans. Inf. Theory **24**, 657 (1978); **25**, 179 (1979); **26**, 78 (1980).
[10] O. Pfister *et al.*, Phys. Rev. Lett. **86**, 4512 (2001).
[11] M. Lewenstein *et al.*, Phys. Rev. Lett. **26**, 3131 (1990); D. Gauthier *et al.*, Phys. Rev. Lett. **68**, 464 (1992).
[12] M. Brune *et al.*, Phys. Rev. A **35**, 154 (1987); M. Brune *et al.*, Phys. Rev. Lett. **59**, 1899 (1987).
[13] C. Ironside, IEEE J. Quantum Electron. **28**, 842 (1992).
[14] D. H. Marti *et al.*, IEEE J. Quantum Electron. **39**, 1066 (2003).
[15] A. Zavriyev *et al.*, Opt. Lett. **20**, 1886 (1995); E. Dupont *et al.*, Appl. Phys. Lett. **65**, 1560 (1994); E. Dupont *et al.*, Phys. Rev. Lett. **74** , 3596 (1995).
[16] L. Narducci *et al.*, Phys. Rev. A **16**, 1665 (1977).
[17] J. Li and C. Z. Ning, Phys. Rev. Lett. **91**, 097401 (2003).
[18] S. Johnson and J. Joannopoulos, *Photonic Crystals* (Kluwer Academic Publishers, Boston, 2002).